

EMC Effect of Tritium and Helium-3 from the JLab MARATHON Experiment

D. Abrams,¹ H. Albataineh,² B. S. Aljawrneh,³ S. Alsalmi,^{4,5} D. Androic,⁶ K. Aniol,⁷ W. Armstrong,⁸ J. Arrington,^{8,9} H. Atac,¹⁰ T. Averett,¹¹ C. Ayerbe Gayoso,¹¹ X. Bai,¹ J. Bane,¹² S. Barcus,¹¹ A. Beck,¹³ V. Bellini,¹⁴ H. Bhatt,¹⁵ D. Bhetuwal,¹⁵ D. Biswas,¹⁶ D. Blyth,⁸ W. Boeglin,¹⁷ D. Bulumulla,¹⁸ J. Butler,¹⁹ A. Camsonne,¹⁹ M. Carmignotto,¹⁹ J. Castellanos,¹⁷ J.-P. Chen,¹⁹ I. C. Cloët,⁸ E. O. Cohen,²⁰ S. Covrig,¹⁹ K. Craycraft,¹¹ R. Cruz-Torres,¹³ B. Dongwi,¹⁴ B. Duran,¹⁰ D. Dutta,¹⁵ N. Fomin,¹² E. Fuchey,²¹ C. Gal,¹ T. N. Gautam,¹⁶ S. Gilad,¹³ K. Gnanvo,¹ T. Gogami,²² J. Gomez,¹⁹ C. Gu,¹ A. Habarakada,¹⁶ T. Hague,⁴ J.-O. Hansen,¹⁹ M. Hattawy,⁸ F. Hauenstein,¹⁸ D. W. Higinbotham,¹⁹ R. J. Holt,^{8,23} E. W. Hughes,²⁴ C. Hyde,¹⁸ H. Ibrahim,²⁵ S. Jian,¹ S. Joosten,¹⁰ A. Karki,¹⁵ B. Karki,²⁶ A. T. Katramatou,⁴ C. Keith,¹⁹ C. Keppel,¹⁹ M. Khachatryan,¹⁸ V. Khachatryan,²⁷ A. Khanal,¹⁷ A. Kievsyky,²⁸ D. King,²⁹ P. M. King,²⁶ I. Korover,³⁰ S. A. Kulagin,³¹ K. S. Kumar,²⁷ T. Kutz,²⁷ N. Lashley-Colthirst,¹⁶ S. Li,³² W. Li,³³ H. Liu,²⁴ S. Liuti,¹ N. Liyanage,¹ P. Markowitz,¹⁷ R. E. McClellan,¹⁹ D. Meekins,¹⁹ S. Mey-Tal Beck,¹³ Z.-E. Meziani,¹⁰ R. Michaels,¹⁹ M. Mihovilovic,^{34,35,36} V. Nelyubin,¹ D. Nguyen,¹ Nuruzzaman,³⁷ M. Nycz,⁴ R. Obrecht,²¹ M. Olson,³⁸ V. F. Owen,¹¹ E. Pace,³⁹ B. Pandey,^{16,*} V. Pandey,⁴⁰ M. Paolone,¹⁰ A. Papadopoulou,¹³ S. Park,²⁷ S. Paul,¹¹ G. G. Petratos,⁴ R. Petti,⁴¹ E. Piassetzky,²⁰ R. Pomatsalyuk,⁴² S. Premathilake,¹ A. J. R. Puckett,²¹ V. Punjabi,⁴³ R. D. Ransome,³⁷ M. N. H. Rashad,¹⁸ P. E. Reimer,⁸ S. Riordan,⁸ J. Roche,²⁶ G. Salmè,⁴⁴ N. Santiesteban,³² B. Sawatzky,¹⁹ A. Schmidt,¹³ B. Schmookler,¹³ S. Scopetta,⁴⁵ J. Segal,¹⁹ E. P. Segarra,¹³ A. Shahinyan,⁴⁶ S. Širca,^{34,35} N. Sparveris,¹⁰ T. Su,^{4,47} R. Suleiman,¹⁹ H. Szumila-Vance,¹⁹ A. S. Tadepalli,³⁷ L. Tang,^{16,19} W. Tireman,⁴⁸ F. Tortorici,¹⁴ G. M. Urciuoli,⁴⁴ B. Wojtsekhowski,¹⁹ S. Wood,¹⁹ Z. H. Ye,^{8,†} Z. Y. Ye,⁴⁹ and J. Zhang²⁷

(Jefferson Lab Hall A Tritium Collaboration)

¹University of Virginia, Charlottesville, Virginia 22904, USA

²Texas A & M University, Kingsville, Texas 78363, USA

³North Carolina A and T State University, Greensboro, North Carolina 27411, USA

⁴Kent State University, Kent, Ohio 44240, USA

⁵King Saud University, Riyadh 11451, Kingdom of Saudi Arabia

⁶University of Zagreb, 10000 Zagreb, Croatia

⁷California State University, Los Angeles, California 90032, USA

⁸Physics Division, Argonne National Laboratory, Lemont, Illinois 60439, USA

⁹Lawrence Berkeley National Laboratory, Berkeley, California 94720, USA

¹⁰Temple University, Philadelphia, Pennsylvania 19122, USA

¹¹William & Mary, Williamsburg, Virginia 23187, USA

¹²University of Tennessee, Knoxville, Tennessee 37996, USA

¹³Massachusetts Institute of Technology, Cambridge, Massachusetts 02139, USA

¹⁴Istituto Nazionale di Fisica Nucleare, Sezione di Catania, 95123 Catania, Italy

¹⁵Mississippi State University, Mississippi State, Mississippi 39762, USA

¹⁶Hampton University, Hampton, Virginia 23669, USA

¹⁷Florida International University, Miami, Florida 33199, USA

¹⁸Old Dominion University, Norfolk, Virginia 23529, USA

¹⁹Jefferson Lab, Newport News, Virginia 23606, USA

²⁰School of Physics and Astronomy, Tel Aviv University, Tel Aviv, Israel

²¹University of Connecticut, Storrs, Connecticut 06269, USA

²²Tohoku University, Sendai 980-8576, Japan

²³California Institute of Technology, Pasadena, California 91125, USA

²⁴Columbia University, New York, New York 10027, USA

²⁵Cairo University, Cairo, Giza 12613 Egypt

²⁶Ohio University, Athens, Ohio 45701, USA

²⁷Stony Brook, State University of New York, New York 11794, USA

²⁸Istituto Nazionale di Fisica Nucleare, Sezione di Pisa, 56127 Pisa, Italy

²⁹Syracuse University, Syracuse, New York 13244, USA

³⁰Nuclear Research Center-Negev, Beer-Sheva 84190, Israel

³¹Institute for Nuclear Research of the Russian Academy of Sciences, 117312 Moscow, Russia

³²University of New Hampshire, Durham, New Hampshire 03824, USA

³³University of Regina, Regina, Saskatchewan S4S 0A2, Canada

³⁴*Faculty of Mathematics and Physics, University of Ljubljana, Ljubljana 1000, Slovenia*³⁵*Jožef Stefan Institute, Ljubljana, Slovenia*³⁶*Institut für Kernphysik, Johannes Gutenberg-Universität, Mainz 55122, Germany*³⁷*Rutgers, The State University of New Jersey, Piscataway, New Jersey 08855, USA*³⁸*Saint Norbert College, De Pere, Wisconsin 54115, USA*³⁹*University of Rome Tor Vergata, 00133 Rome, Italy*⁴⁰*Center for Neutrino Physics, Virginia Tech, Blacksburg, Virginia 24061, USA*⁴¹*University of South Carolina, Columbia, South Carolina 29208, USA*⁴²*Institute of Physics and Technology, 61108 Kharkov, Ukraine*⁴³*Norfolk State University, Norfolk, Virginia 23504, USA*⁴⁴*Istituto Nazionale di Fisica Nucleare, Sezione di Roma, 00185 Rome, Italy*⁴⁵*University of Perugia and INFN, Sezione di Perugia, 06123 Perugia, Italy*⁴⁶*Yerevan Physics Institute, Yerevan 375036, Armenia*⁴⁷*Shandong Institute of Advanced Technology, Jinan, Shandong 250100, China*⁴⁸*Northern Michigan University, Marquette, Michigan 49855, USA*⁴⁹*University of Illinois-Chicago, Chicago, Illinois 60607, USA* (Received 19 September 2024; revised 22 May 2025; accepted 8 July 2025; published 7 August 2025)

Measurements of the EMC effect in the tritium and helium-3 mirror nuclei are reported. The data were obtained by the MARATHON Jefferson Lab experiment, which performed deep inelastic electron scattering from deuterium and the three-body nuclei, using a cryogenic gas target system and the high resolution spectrometers of the Hall A Facility of the Lab. The data cover the Bjorken x range from 0.20 to 0.83, corresponding to a squared four-momentum transfer Q^2 range from 2.7 to 11.9 (GeV/c)², and to an invariant mass W of the final hadronic state greater than 1.84 GeV/c². The tritium EMC effect measurement is the first of its kind. The MARATHON experimental results are compared to results from previous measurements by DESY-HERMES and JLab–Hall C experiments, as well as with few-body theoretical predictions.

DOI: [10.1103/PhysRevLett.135.062502](https://doi.org/10.1103/PhysRevLett.135.062502)

The European Muon Collaboration (EMC) discovered a significant suppression of the electron deep inelastic scattering (DIS) cross section (or equivalently the structure function F_2) for iron per nucleon with respect to that of deuterium for the Bjorken scaling variable x from 0.3 to 0.7, corresponding to the quark-valence region [1]. Bjorken x is defined in the lab frame as $x = Q^2/[2M(E - E')]$, where M is the nucleon mass, and E and E' are the incident and scattered lepton energies in the scattering from the nucleus. This effect, named *EMC effect*, was confirmed by a reanalysis of older SLAC data [2], and by various experiments with electron and muon beams [3–6]. Nuclear effects are commonly studied using the ratio $R_A = \sigma_A/\sigma_d$ of cross sections for scattering off a nucleus A and deuterium d , normalized per nucleon. In the valence quark region $0.3 < x < 0.6$, R_A is approximately a linear function of x with negligible Q^2 dependence. The slope dR_A/dx in this region depends on the nuclear target and its value increases with the nuclear mass number A . Nuclear effects

on R_A have also been studied in other kinematical regions. (For a review of data and models see Refs. [7–11]).

In the infinite momentum frame, x can be interpreted in DIS as the fraction of the target nucleon’s momentum carried by the struck quark. Momentum conservation suggests that if the valence quark fraction distribution is suppressed in nuclei then the corresponding lower- x fraction in the total distribution should be enhanced. Quite a few models have been suggested to explain the redistribution of missing valence light-cone momentum in nuclei between bound nucleons and nonnucleon degrees of freedom in nuclei such as nuclear pions, nucleon resonances, multiquark clusters, and change of the quark-gluon confinement scale in nuclear environment. (For a review see Refs. [7–11].) It has been known since the 1970s that smearing the nucleon structure function with the nuclear momentum distribution (due to Fermi motion) results in an enhancement of the nuclear structure functions at high x [12,13]. The available EMC-effect data have shown this enhancement, but also a significant suppression for x up to about 0.7. A revision of the Fermi motion correction to include the effect of the nuclear binding allows a reduction of the discrepancy between calculations and data [14]. Further refinements and quantitative studies of the Fermi motion and nuclear binding with a realistic nuclear spectral function, including a high-momentum component, can

*Present address: Department of Physics and Astronomy, Virginia Military Institute, Lexington, Virginia 24450, USA.

†Present address: Department of Physics, Tsinghua University, Beijing 100084, China.

explain about half of the observed EMC effect at its maximum value around $x \sim 0.7$ [15–17], somewhat underestimating the value of the slope dR_A/dx for $0.3 < x < 0.7$.

Since bound nucleons are off mass shell due to the nuclear binding, their invariant mass squared is, for kinematic reasons, less than M^2 . This off-shell effect results in a nuclear modification to the structure of the bound nucleons, after averaging with the nuclear energy-momentum distribution [18]. In the theoretical model of Ref. [17] this effect is addressed in terms of a dimensionless function $\delta f(x)$ describing the relative off-shell correction to the nucleon F_2 structure function. There it was shown that the EMC effect can be described with high accuracy over the complete kinematic region covered by existing data using the same $\delta f(x)$ function for bound protons and neutrons. Predictions based on this assumption were verified with a broad range of data from a variety of high-energy processes [19–21]. Further study of a possible isospin dependence [20,22] of this correction requires the use of nuclei with a large neutron or proton excess like ${}^3\text{H}$ and ${}^3\text{He}$. Nuclear modifications of various types of the bound nucleon structure in the valence quark region are also present in a number of different models [23–25]. Other nuclear effects, such as corrections from meson-exchange currents and the propagation of the hadronic (quark-gluon) component of the virtual intermediate photon in the nuclear environment are relevant in the small x region [7–9,26].

A crucial step in understanding the origin of the EMC effect is a comparison of realistic calculations of the structure functions of the lightest nuclei, deuterium [${}^2\text{H}$], helium-3 [${}^3\text{He}$ (h)], and tritium [${}^3\text{H}$ (t)], with precision measurements. In this Letter we report the measurement of the EMC effect of the $A = 3$ mirror nuclei by the MARATHON Jefferson Lab (JLab) experiment [27], which previously determined the ratio of the proton (p) and neutron (n) F_2 structure functions, F_2^n/F_2^p , from DIS measurements off tritons (t) and helions (h) [28]. MARATHON used the Continuous Electron Beam Accelerator and the Hall A Facility [29] of JLab.

Electrons scattered from d , h , and t nuclei in high-pressure, cryogenic gas target cells [30], cooled to a temperature of 40 K, were detected in the Left and Right High Resolution Spectrometers (HRS) of the Hall [29]. The incident-beam energy was fixed at 10.59 GeV, and the beam current ranged from 14.6 to 22.5 μA . The Left HRS was operated at a fixed momentum of 3.1 GeV/ c , placed at angles between 16.8° and 33.6° . The Right HRS was operated at a single setting of 2.9 GeV/ c and 36.1° . In each HRS system, particles were detected using two planes of scintillators for event triggering, a pair of drift chambers for track reconstruction, and a gas threshold Cherenkov counter and a lead-glass calorimeter for electron identification. At each kinematic setting, the target cells were cycled every few hours in the beam in order to minimize effects of a possible time dependence of

the stability (“drift”) of the beam diagnostic or other instrumentation (e.g., the beam current monitors). Essential information for the experimental apparatus has been provided in Ref. [28]. Additional detailed information on the Hall A spectrometer facility, and the associated beam instrumentation with calibrations, as used in MARATHON, are given in Refs. [31–36].

All events identified as electrons originating from the gas inside each target cell were binned by Bjorken x , resulting in the formation of an electron yield, equal to the number of scattered electrons for each bin divided by the number of incident beam electrons and of gas target nuclei per unit area, as described in Ref. [28]. The ratio of the yields for two targets is equivalent to the ratio of their cross sections, because the associated identical target lengths [28] and spectrometer acceptances cancel out in the latter ratio. The overall electron detection efficiency, close to unity (~ 0.985), was found to be independent of the target cell at all kinematics, so it also cancels out in the ratios of the yields. Several multiplicative correction factors were applied to the individual target yields. (i) The correction for computer dead time ranged from 1.001 to 1.065; (ii) target density change due to beam heating effects ranged from 1.066 to 1.112; (iii) falsely reconstructed events originating from the end caps ranged from 0.973 to 0.998; (iv) background events originating from charge-symmetric processes ranged from 0.986 to 0.999; (v) radiative effects ranged from 0.853 to 1.167; (vi) beta decay of tritons to helions (applicable only to the tritium yield) ranged from 0.997 at the beginning to 0.989 at the end of the experiment; (vii) Coulomb distortion effects ranged from 0.997 to 1.000; and (viii) bin-centering adjustment ranged from 0.995 to 1.001. In the above, the ranges refer to the ${}^3\text{He}$, ${}^3\text{H}$, and ${}^2\text{H}$ gas yields. A cross section model from Refs. [17,19] was adopted for the Coulomb correction (which used the Q^2 -effective approximation as outlined in Ref. [37]), and for the bin-centering correction.

Although the corrections to the individual cross sections may be sizeable, the total correction to the ratio of cross sections, such σ_h/σ_d and σ_t/σ_d , is much smaller because of partial cancellation of the corrections. Likewise, in some cases the associated systematic uncertainties also partially cancel in the ratios of cross sections. For example, the radiative effect correction to the above two ratios ranges only from 1.000 to 1.004 and 1.006 to 1.012, respectively. The dominant point-to-point systematic uncertainties for the yield ratios are those from the beam-heating gas target density changes [$\pm(0.1\% - 0.5\%)$], the radiative correction [$\pm(0.25\% - 0.45\%)$], and the choice of spectrometer acceptance limits ($\pm 0.2\%$). The total point-to-point uncertainty ranges from $\pm 0.46\%$ to $\pm 0.49\%$ for the σ_h/σ_d ratio, and $\pm 0.34\%$ to $\pm 0.47\%$ for the σ_t/σ_d ratio. Details on the determination of the yields, the associated corrections and uncertainties, and other relevant subjects can be found in Refs. [31–36].

The experiment also collected DIS data for the proton, in the x range from 0.20 to 0.38, for normalization purposes. The resulting σ_d/σ_p ratio measured by MARATHON is in excellent agreement with the reference measurements of the seminal SLAC-E49b and E87 experiments [38], as shown in Ref. [28]. The σ_d/σ_p data from MARATHON allowed for an accurate determination of the $R_{np} = \sigma_n/\sigma_p$ ratio from the relation [19,39] $R_{np} = (\sigma_d/\sigma_p)/R_d - 1$, where $R_d = \sigma_d/(\sigma_p + \sigma_n)$.

In the extraction of R_{np} from the MARATHON ^3He and ^3H data, it was realized [28] that the σ_h/σ_t ratio had to be normalized by a factor of 1.025, as a result of requiring the equality of the R_{np} values extracted from σ_h/σ_t and σ_d/σ_p in the vicinity of $x = 0.3$. In the work described in this Letter we follow the same approach by requiring that the R_{np} value extracted individually from σ_t/σ_d and σ_h/σ_d be equal to that extracted from σ_d/σ_p in the vicinity of $x = 0.3$, where nuclear corrections are minimal. We define the EMC-type ratios for the cross sections of ^3He (h) and ^3H (t) as $R_h = \sigma_h/(2\sigma_p + \sigma_n)$ and $R_t = \sigma_t/(\sigma_p + 2\sigma_n)$, respectively. Then, the double ratios $\mathcal{R}_{hd} = R_h/R_d$ and $\mathcal{R}_{td} = R_t/R_d$ allow for the determination of R_{np} in two separate ways:

$$R_{np} = \frac{2\mathcal{R}_{hd}(\sigma_d/\sigma_h) - 1}{1 - \mathcal{R}_{hd}(\sigma_d/\sigma_h)} = \frac{\mathcal{R}_{td}(\sigma_d/\sigma_t) - 1}{1 - 2\mathcal{R}_{td}(\sigma_d/\sigma_t)}, \quad (1)$$

once the ratios σ_h/σ_d and σ_t/σ_d have been measured experimentally, and the ratios \mathcal{R}_{hd} and \mathcal{R}_{td} can be calculated using a reliable theoretical model.

The values for the R_d , \mathcal{R}_{hd} , and \mathcal{R}_{td} ratios employed in this Letter were obtained prior to the analysis of the MARATHON data from the theoretical model of Kulagin and Petti (K-P) [17,19], which provides a very good description of the EMC effect for all known targets (for a review see Ref. [26]). This model includes a number of nuclear effects out of which the major correction for the relevant kinematics comes from the smearing effect with the nuclear energy-momentum distribution, described in terms of the nuclear spectral function, together with an off-shell correction to the bound nucleon cross sections [17]. The underlying nucleon structure functions come from a global QCD analysis [40], which was performed up to NNLO approximation in the strong coupling constant including target mass corrections [41] as well as those due to higher-twist effects (OPE [41]). For the spectral functions of the ^3H and ^3He nuclei, the results of Ref. [39] have been used, while for the ^2H wave function the Argonne AV18 nucleon-nucleon interaction [42] was applied. In order to evaluate theoretical uncertainties, the ^3He spectral function of Ref. [43] and the Bonn ^2H wave function of Ref. [44] were used. Reasonable variations of the high-momentum part of the nucleon momentum distribution in ^3H and ^3He were considered, and uncertainties

in the off-shell correction of Ref. [17], as well as in the nucleon structure functions of Ref. [40], were accounted for [45].

The comparison of R_{np} as extracted from the measured σ_h/σ_d , σ_t/σ_d , and σ_d/σ_p ratios was actually done at $x = 0.31$, where nuclear corrections are not expected to contribute to isoscalar nuclear ratios such as \mathcal{R}_{hd} , \mathcal{R}_{td} , and R_d . This expectation is based on the experimental data for $A \geq 3$ nuclei [3–6] in the range $0.25 \leq x \leq 0.35$, taking into account the quoted normalization uncertainties therein. This approach is also in line with the results of Refs. [19,46]. The K-P model predicts a value of 1.000 at $x = 0.31$ for \mathcal{R}_{hd} , \mathcal{R}_{td} , and R_d , with uncertainties of $\pm 0.38\%$, $\pm 0.42\%$ and $\pm 0.20\%$, respectively. The above value for R_d is in very good agreement with the independent analyses of Refs. [3,25,47,48]. The values of σ_d/σ_p , σ_h/σ_d , and σ_t/σ_d at $x = 0.31$ were determined by weighted fits to the three corresponding sets [x between 0.20 and 0.83 (0.20 and 0.38) for σ_h/σ_d and σ_t/σ_d (σ_d/σ_p)], which included statistical and point-to-point uncertainties added in quadrature.

Because the extracted σ_n/σ_p ratio must be the same from each set of nuclei, the σ_h/σ_d and σ_t/σ_d ratios at $x = 0.31$ were normalized by a multiplicative factor of 1.021 ± 0.005 and 0.996 ± 0.005 , respectively. These two factors are consistent with the normalization factor of 1.025 ± 0.007 of the σ_h/σ_t ratio, as determined similarly in Ref. [28]. All values for the σ_h/σ_d and σ_t/σ_d ratios reported and further used in this Letter have been normalized using these two factors. The normalized ratios' values are given in Tables I and II of Supplemental Material [49] together with associated uncertainties, and plotted in Fig. 1. As a matter of convention, which will be followed for the remainder of this Letter, the ratios have been adjusted so that the cross sections are per nucleon.

The data are compared to the theoretical predictions of the K-P model [19,45] and the model of Tropicano *et al.* (TEMS) [22]. Both K-P and TEMS predictions are based on a nuclear convolution approach [17,19,51], but they involve different assumptions. As mentioned above, K-P use the proton and neutron structure functions from a global QCD fit [40] and the relative off-shell effect (OSE) correction from Ref. [17]. The TEMS group employs the results of the CJ15 analysis [52] with the OSE correction adjusted from a fit to JLab Hall C σ_h/σ_d data [6], allowing for different off-shell modifications for bound protons and neutrons. The latter data are also shown in Fig. 1 for W^2 values greater than $3.4 \text{ (GeV}/c^2)^2$. Here, it should be noted that in order for the Hall C data to provide values of σ_n/σ_p which would match those of MARATHON, they should be adjusted upwards by about 2.5%. Such a requirement would make the two σ_h/σ_d data sets mutually consistent. The MARATHON results are in excellent agreement with the K-P prediction over the entire measured range of x , as quantified by a χ^2 per degree of freedom of 1.0, and with

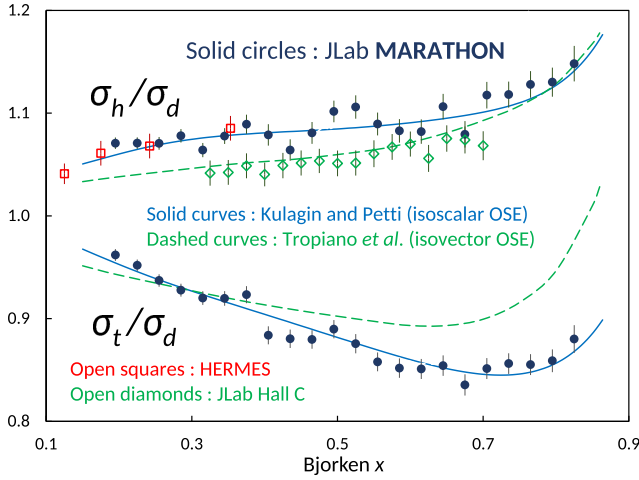


FIG. 1. The MARATHON results on the ${}^3\text{He}/{}^2\text{H}$ and ${}^3\text{H}/{}^2\text{H}$ DIS cross section ratios as a function of Bjorken x . The solid curves are the prediction of the K-P model (with isoscalar OSE) [19,45], and the dashed curves are the result of Tropiano *et al.* (with isovector OSE) [22]. Also shown are overlapping results from the HERMES experiment [5], as binned in Ref. [50], and final results from JLab Experiment E03-103 [6] (see text). The error bars include statistical and point-to-point systematics uncertainties, added in quadrature.

overlapping results from the DESY-HERMES experiment [5], as binned in Ref. [50], also shown in Fig. 1.

The arithmetic mean of σ_h/σ_d and σ_t/σ_d provides a model-independent determination of the average isoscalar EMC effects of the three-body mirror nuclei ${}^3\text{He}$ and ${}^3\text{H}$. The resulting isoscalar ratio $(\sigma_h + \sigma_t)/(2\sigma_d)$ values and associated uncertainties are listed in Table III of Ref. [49], and plotted in Fig. 2 along with statistical and point-to-point systematic uncertainties added in quadrature. Also shown is the result for $A = 3$ of the SLAC-E139 parametrization of the EMC effect [in terms of $\ln(A)$] [3], and the predictions of K-P [19,45] and TEMS [22], as well as the results of calculations by Segarra *et al.* [25] and Fornetti *et al.* [53]. The former is based on a parameterization of the EMC effect in terms of the fraction of the nuclear high-momentum component generated by short-range correlations. The latter is based on a Poincaré covariant approach, using light-front Hamiltonian dynamics and wave functions obtained from modern nuclear interactions models.

To obtain the isoscalar EMC effect separately for the ${}^3\text{H}$ and ${}^3\text{He}$ nuclei, the ratios σ_t/σ_d and σ_h/σ_d must be corrected for the neutron and proton excess, respectively. This is achieved by multiplying them by the customary factor

$$F_{\text{iso}} = \frac{A(1 + R_{np})}{2[Z + (A - Z)R_{np}]}, \quad (2)$$

where Z is the nuclear charge number. The $R_{np} = \sigma_n/\sigma_p$ values used in Eq. (2) are the ones measured by the

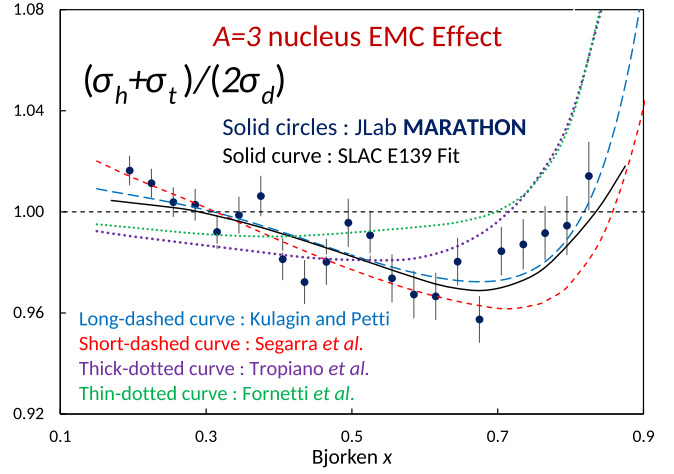


FIG. 2. The $A = 3$ EMC effect in a isoscalar combination of the ${}^3\text{He}$ and ${}^3\text{H}$ cross sections as a function of Bjorken x . The error bars include statistical and point-to-point systematics uncertainties. The long-dashed curve is the prediction of the K-P model [19,45] (with isoscalar OSE), the thick-dotted, dashed, and thin-dotted curves are results from Refs. [22] (TEMS, with isovector OSE), [25], and [53], respectively. The solid curve shows the A -dependent SLAC-E139 parametrization [3].

MARATHON experiment and reported in Ref. [28]. The values of the correction are listed in Tables IV and V of Ref. [49]. For ${}^3\text{He}$, they range from 0.949 (lowest x) to 0.888 (highest x). For ${}^3\text{H}$, they range from 1.057 (lowest x) to 1.144 (highest x). Using the MARATHON-extracted R_{np} [i.e., substituting $R_{np} = F_2^n/F_2^p$ as given by Eq. (2) of Ref. [28] in the above Eq. (2)] allows us to cast the two isoscalar EMC ratios as follows:

$$(\sigma_h/\sigma_d)_{\text{iso}} = \frac{1}{2}[\sigma_h/\sigma_d + \mathcal{R}_{ht}(\sigma_t/\sigma_d)], \quad (3)$$

$$(\sigma_t/\sigma_d)_{\text{iso}} = \frac{1}{2}[\sigma_t/\sigma_d + (\sigma_h/\sigma_d)/\mathcal{R}_{ht}], \quad (4)$$

where the “super-ratio” $\mathcal{R}_{ht} = R_h/R_t$ is the ratio of the previously defined R_h and R_t ratio quantities, and for which the K-P model prediction is used [19,28]. The values of \mathcal{R}_{ht} are listed, along with their estimated theory uncertainties, in Ref. [28], where it can be seen that the deviation of \mathcal{R}_{ht} from unity is well below 1% for most points, with a maximal value reaching 1.25%. Note that $(\sigma_h/\sigma_t)_{\text{iso}} = \mathcal{R}_{ht}$, and in the limit $\mathcal{R}_{ht} = 1$ we have identical individual isoscalar EMC-effects for ${}^3\text{H}$ and ${}^3\text{He}$.

The measured values of $(\sigma_h/\sigma_d)_{\text{iso}}$ and $(\sigma_t/\sigma_d)_{\text{iso}}$ of the individual EMC effects of the two $A = 3$ nuclei are given in Tables IV and V, respectively, of Ref. [49], together with associated uncertainties, and plotted in Fig. 3. Since the ratios σ_h/σ_d and σ_t/σ_d are correlated, the uncertainties of the three $A = 3$, ${}^3\text{H}$, and ${}^3\text{He}$ EMC effects have been determined by a Monte Carlo simulation, where it has been

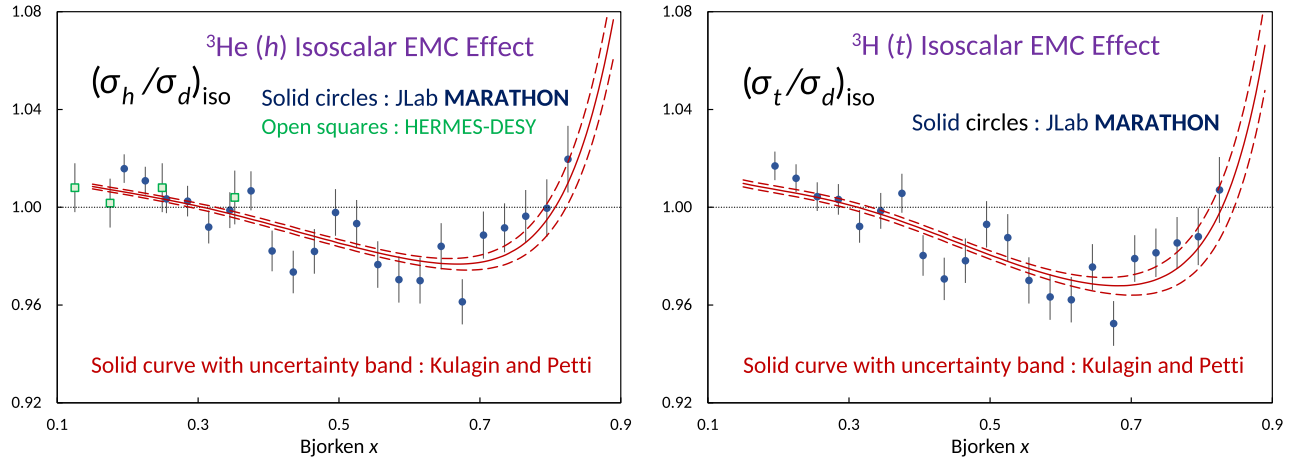


FIG. 3. Left: the ${}^3\text{He}/{}^2\text{H}$ cross section ratio from the MARATHON experiment corrected for isoscalarity as a function of Bjorken x . Also shown are overlapping results from the HERMES experiment [5], as binned in Ref. [50]. Right: the ${}^3\text{H}/{}^2\text{H}$ cross section ratio from the MARATHON experiment corrected for isoscalarity as a function of Bjorken x . For both plots, the error bars include statistical and point-to-point systematic uncertainties, added in quadrature. The solid curves with uncertainty bands are the predictions of the K-P model [19,45].

estimated that one half of both the point-to-point and overall scale uncertainties of the two ratios are correlated. A model is used for each EMC effect and then its uncertainty (statistical or systematic) is the root mean square deviation between the model and the randomized simulated values. The essence of such simulation is that the same random deviation is used to account for the uncertainty of the deuteron yield, which appears twice in the functional form of each ratio. Also, shown in both panels of Fig. 3 are the predictions of K-P model [19,45], and in the left panel overlapping results from the HERMES experiment [5], as binned in Ref. [50], which are in excellent agreement with the MARATHON ones. The JLab Hall C data [6], which are consistent with the MARATHON data within overall normalizations, are not shown as they have been determined with different isoscalarity correction. (The isoscalarity corrections of the MARATHON and HERMES data are mutually consistent.)

It is customary to extract the slope of $(\sigma_A/\sigma_d)_{\text{iso}}$ in the x range between 0.3 and 0.7 from EMC measurements, assuming that the effect follows an approximate linear behavior in this range. A linear fit to the MARATHON data including statistical and point-to-point systematic uncertainties results in the values of -0.085 ± 0.037 and -0.10 ± 0.04 for ${}^3\text{He}$ and ${}^3\text{H}$ slopes, respectively. The ${}^3\text{He}$ slope value is similar to the -0.085 ± 0.027 one from the JLab Hall C data [6], although it uses different isoscalarity correction factor values than MARATHON.

In summary, the MARATHON experiment has provided the first measurement of the EMC effect of the tritium nucleus at four momentum transfers in the DIS regime, with $0.20 < x < 0.83$. It has also extended the kinematical range of existing measurements on the EMC effect of ${}^3\text{He}$, up to x values greater than 0.8 with $Q^2 > 10$ (GeV/c) 2 .

The extracted isoscalar combination of the ${}^3\text{H}$ and ${}^3\text{He}$ data have provided the EMC effect for an $A = 3$ nucleus which is consistent with the A -dependent SLAC-E139 parametrization based on measurements for $A \geq 4$ nuclei [3]. The new data are in agreement with theoretical predictions in which nuclear corrections originate from the energy-momentum distribution of bound nucleons together with an off-shell modification of their internal structure [17,19], but they do not provide evidence for isovector off-shell effects for bound nucleons in the three-nucleon nuclei as argued in Ref. [22]. The new data are expected to provide unique input for QCD studies of the nucleons, and of the partonic structure of the few-body nuclear systems in the valence quark region, including the effects owed to the higher-twist QCD corrections.

Acknowledgments—We acknowledge the outstanding support of the staff of the Accelerator Division and Hall A Facility of JLab, and work of the staff of the Savannah River Tritium Enterprises and the JLab Target Group. We thank Dr. M. E. Christy and Dr. Y. Kolomensky for useful discussions on the optical properties of the HRS systems, and the interpretation of the data, respectively. We thank Dr. Gunar Schnell for clarifications on the HERMES-DESY ${}^3\text{He}$ DIS data. We are grateful to Dr. W. Melnitchouk for his contributions to the development of the MARATHON proposal, and to Dr. A. W. Thomas for many valuable discussions on and support of the MARATHON project since its inception. This material is based upon work supported by the U.S. Department of Energy (DOE), Office of Science, Office of Nuclear Physics under Contracts No. DE-AC05-06OR23177 and No. DE-AC02-06CH11357. This work was also supported DOE Contract No. DE-AC02-05CH11231, DOE Awards

DE-SC0016577 and DE-SC0010073, National Science Foundation Awards NSF-PHY-1405814 and NSF-PHY-1714809, the Kent State University Research Council, the PAZY Foundation and the Israeli Science Foundation under Grants No. 136/12 and No. 1334/16, by the Science Committee of the Republic of Armenia under Grant No. 21AG-1C085, and the Italian Institute of Nuclear Physics.

Authored by Jefferson Science Associates, LLC under U.S. DOE Contracts DE-AC05-06OR23177 and DE-AC02-06CH11357. The U.S. Government retains a nonexclusive, paid-up, irrevocable, worldwide license to publish or reproduce this manuscript for U.S. Government purposes.

-
- [1] J. J. Aubert *et al.*, *Phys. Lett.* **123B**, 275 (1983).
 [2] A. Bodek *et al.*, *Phys. Rev. Lett.* **50**, 1431 (1983); **51**, 534 (1983).
 [3] R. G. Arnold *et al.*, *Phys. Rev. Lett.* **52**, 727 (1984); J. Gomez *et al.*, *Phys. Rev. D* **49**, 4348 (1994).
 [4] P. Amaudruz *et al.*, *Nucl. Phys.* **B441**, 3 (1995).
 [5] K. Airapetian *et al.*, *Phys. Lett. B* **567**, 339 (2003).
 [6] J. Seely *et al.*, *Phys. Rev. Lett.* **103**, 202301 (2009); J. Arrington *et al.*, *Phys. Rev. C* **104**, 065203 (2021).
 [7] M. Arneodo, *Phys. Rep.* **240**, 301 (1994).
 [8] D. F. Geesaman, K. Saito, and A. W. Thomas, *Annu. Rev. Nucl. Part. Sci.* **45**, 337 (1995).
 [9] P. R. Norton, *Rep. Prog. Phys.* **66**, 1253 (2003).
 [10] Simone Malace, David Gaskell, Douglas W. Higinbotham, and Ian C. Cloet, *Int. J. Mod. Phys. E* **23**, 1430013 (2014).
 [11] O. Hen, G. A. Miller, E. Piassetzky, and L. B. Weinstein, *Rev. Mod. Phys.* **89**, 045002 (2017).
 [12] G. B. West, *Ann. Phys. (N.Y.)* **74**, 464 (1972); W. B. Atwood and G. B. West, *Phys. Rev. D* **7**, 773 (1973).
 [13] A. Bodek and J. L. Ritchie, *Phys. Rev. D* **23**, 1070 (1981).
 [14] S. V. Akulinichev, S. A. Kulagin, and G. M. Vagradov, *Phys. Lett.* **158B**, 485 (1985); S. V. Akulinichev, S. Shlomo, S. A. Kulagin, and G. M. Vagradov, *Phys. Rev. Lett.* **55**, 2239 (1985).
 [15] S. A. Kulagin, *Nucl. Phys.* **A500**, 653 (1989).
 [16] C. Ciofi Degli Atti and S. Liuti, *Phys. Lett. B* **225**, 215 (1989).
 [17] S. A. Kulagin and R. Petti, *Nucl. Phys.* **A765**, 126 (2006).
 [18] S. A. Kulagin, G. Piller, and W. Weise, *Phys. Rev. C* **50**, 1154 (1994).
 [19] S. A. Kulagin and R. Petti, *Phys. Rev. C* **82**, 054614 (2010).
 [20] S. A. Kulagin and R. Petti, *Phys. Rev. C* **90**, 045204 (2014).
 [21] P. Ru, S. A. Kulagin, R. Petti, and B. W. Zhang, *Phys. Rev. D* **94**, 113013 (2016).
 [22] A. J. Tropiano, J. J. Ethier, W. Melnitchouk, and N. Sato, *Phys. Rev. C* **99**, 035201 (2019).
 [23] L. L. Frankfurt and M. I. Strikman, *Nucl. Phys.* **B250**, 143 (1985).
 [24] I. C. Cloet, W. Bentz, and A. W. Thomas, *Phys. Lett. B* **642**, 210 (2006).
 [25] E. P. Segarra, A. Schmidt, T. Kutz, D. W. Higinbotham, E. Piassetzky, M. Strikman, L. B. Weinstein, and O. Hen, *Phys. Rev. Lett.* **124**, 092002 (2020).
 [26] S. A. Kulagin, *EPJ Web Conf.* **138**, 01006 (2017).
 [27] G. G. Petratos *et al.*, JLab PR12-10-103, MARATHON proposal: Measurement of the F_2^n/F_2^p , d/u Ratios and $A = 3$ EMC effect in deep inelastic electron scattering off the tritium and helium mirror nuclei (2010).
 [28] D. Abrams *et al.* (Jefferson Lab Hall A Tritium Collaboration), *Phys. Rev. Lett.* **128**, 132003 (2022).
 [29] J. Alcorn *et al.*, *Nucl. Instrum. Methods Phys. Res., Sect. A* **522**, 294 (2004).
 [30] R. J. Holt *et al.*, Conceptual design of a tritium gas target for JLab, JLab Report, 2010; D. Meekins, Hall a tritium target, JLab Report, 2018; S. N. Santiesteban *et al.*, *Nucl. Instrum. Methods Phys. Res., Sect. A* **940**, 351 (2019).
 [31] J. Bane, Ph.D. Thesis, University of Tennessee, 2019.
 [32] T. Hague, Ph.D. Thesis, Kent State University, 2020.
 [33] T. Kutz, Ph.D. Thesis, Stony Brook University, 2019.
 [34] H. Liu, Ph.D. Thesis, Columbia University, 2020.
 [35] M. Nycz, Ph.D. Thesis, Kent State University, 2020.
 [36] T. Su, Ph.D. Thesis, Kent State University, 2020.
 [37] Herbert Uberall, *Electron Scattering from Complex Nuclei* (Academic Press, New York, 1971).
 [38] A. Bodek *et al.*, *Phys. Rev. D* **20**, 1471 (1979).
 [39] E. Pace, G. Salmè, S. Scopetta, and A. Kievsky, *Phys. Rev. C* **64**, 055203 (2001).
 [40] S. Alekhin, S. A. Kulagin, and R. Petti, *AIP Conf. Proc.* **967**, 215 (2007).
 [41] H. Georgi and H. D. Politzer, *Phys. Rev. D* **14**, 1829 (1976).
 [42] R. B. Wiringa, V. G. J. Stoks, and R. Schiavilla, *Phys. Rev. C* **51**, 38 (1995); S. Veerasamy and W. N. Polyzou, *Phys. Rev. C* **84**, 034003 (2011).
 [43] R. W. Schulze and P. U. Sauer, *Phys. Rev. C* **48**, 38 (1993).
 [44] R. Machleidt, *Phys. Rev. C* **63**, 024001 (2001).
 [45] Sergey Kulagin and Roberto Petti (private communication).
 [46] L. B. Weinstein, E. Piassetzky, D. W. Higinbotham, J. Gomez, O. Hen, and R. Shneor, *Phys. Rev. Lett.* **106**, 052301 (2011).
 [47] K. A. Griffioen *et al.*, *Phys. Rev. C* **92**, 015211 (2015).
 [48] S. I. Alekhin, S. A. Kulagin, and R. Petti, *Phys. Rev. D* **96**, 054005 (2017).
 [49] See Supplemental Material at <http://link.aps.org/supplemental/10.1103/31xz-s84d> for (i) the kinematical parameters of the measurements, (ii) the ratios of the measured DIS cross sections for the 3 targets (deuterium, helium-3, and tritium), (iii) the ratios of the same cross sections corrected for isoscalarity, and (iv) the associated statistical, systematic and total uncertainties. (All tabulated quantities are described in the main text of the paper.)
 [50] Erika Garutti, Ph.D. Thesis, University of Amsterdam, 2003.
 [51] S. A. Kulagin and W. Melnitchouk, *Phys. Rev. C* **78**, 065203 (2008).
 [52] A. Accardi, L. T. Brady, W. Melnitchouk, J. F. Owens, and N. Sato, *Phys. Rev. D* **93**, 114017 (2016).
 [53] E. Pace, M. Rinaldi, G. Salmè, and S. Scopetta, *Phys. Lett. B* **839**, 137810 (2023); F. Fornetti, E. Pace, M. Rinaldi, G. Salmè, S. Scopetta, and M. Viviani, *Phys. Lett. B* **851**, 138587 (2024).